



Ligand- and structure-based virtual screening of 16-((diisobutylamino)methyl)-6 α -hydroxyvouacapane-7 β ,17 β -lactone, a compound with potential anti-prostate cancer activity

RAÍ C. SILVA^{1,2*}, JOÃO G. C. POIANI³, RYAN S. RAMOS², JOSIVAN S. COSTA², CARLOS H. T. P. SILVA^{2,3}, DAVI S. B. BRASIL^{1,2} and CLEYDSON B. R. SANTOS^{1,2}

¹Postgraduate Program in Medicinal Chemistry and Molecular Modeling, Federal University of Pará, Rua Augusto Corrêa 01, 66075–110, Belém, Pará, Brazil, ²Laboratory of Modeling and Computational Chemistry, Federal University of Amapá, Rod JK Km 2, 68902–280, Macapá, Amapá, Brazil and ³Laboratory of Pharmaceutical Chemistry, Faculty of Pharmaceutical Sciences of Ribeirão Preto, University of São Paulo, Av. Prof. do Café, s/n – Monte Alegre, 14040–903, Ribeirão Preto, São Paulo, Brazil

(Received 29 January, revised 13 May, accepted 29 May 2018)

Abstract: Prostate cancer is one of the leading causes of disease and death on the planet. The probable bioactive pose of 16-((diisobutylamino)methyl)-6 α -hydroxyvouacapane-7 β ,17 β -lactone (N,N-DHL), a pivot compound with prostatic anti-cancer activity, was investigated via a semi-empirical method (PM3) and refined with the base set 6-31+G(d,p) calculated in the DFT method at the B3LYP level of theory. This structure was used in ligand-based virtual screening for five commercial compound bases using the software ROCS and EON that selected 2000 per base and another that resulted in 100 per base, respectively. This set was used for pharmacokinetic and toxicological predictions. The molecular overlap index at 50 % steric/electrostatic provided 68 structures that were used for a molecular docking study. The results showed that of 238,922 structures, only eight, **7** (-10.9 kcal mol $^{-1}$) as the best in the series and **1** (-8.1 kcal mol $^{-1}$) as less favorable, with others in this range (± 2.8 kcal mol $^{-1}$) with their respective binding affinity: **8** (-8.2 kcal mol $^{-1}$), **5** (-8.2 kcal mol $^{-1}$), **4** (-8.3 kcal mol $^{-1}$), **2** (-8.5 kcal mol $^{-1}$), **3** (-8.6 kcal mol $^{-1}$) and **6** (-8.8 kcal mol $^{-1}$) remaining in the final selection. The predictions for 21 pharmacokinetic properties were within the recommended range, similar to 95 % of the drugs available on the market, with no toxicity warning. The structures showed similarity greater than 75 % to the pivot based on binding affinity and predictions but only the structures **6** and **7** were considered more promising for their potential anti-prostate cancer activity (PC-3).

Keywords: dihydrotestosterone; androgen receptor; DFT/6-31+G (d,p); virtual screening; derivative of vouacapane; drug design.

*Corresponding author. E-mail: camposchemistry@gmail.com
<https://doi.org/10.2298/JSC180129047S>

INTRODUCTION

Prostate cancer (PC) is characterized by excessive growth of the prostate, with consequent reduction in the volume and intensity of the urinary stream, being one of the main causes of illness and death in the world.¹ It is the fourth type of cancer with great incidence on Earth, affecting around 1.1 million people.^{2,3} It is estimated that by 2030, the PC will reach 1.7 million new cases and 499000 new deaths, the progress is due, among other reasons, to the growth and aging of the world population.^{4,5} The androgen hormone testosterone (TST) is converted to dihydrotestosterone (DHT) in the stroma and basal cells by the intracellular enzyme 5 α -reductase (5 α R). DHT plays an effective role in the development and growth of the prostate. The androgen receptor has a 10 times greater affinity for DHT than for testosterone.^{6,7}

The species *Pterodon emarginatus* Vogel of the family Fabaceae (synonym of *Pterodon pubescens* Benth.), commonly called “white sucupira” or “faveira”, is a fruit-bearing vegetable.^{8,9} Previous studies, starting from hexane extracts of these fruits, isolated 6 α ,7 β -dihydroxyivoucapan-17 β -oic acid (ADV), with some of its derivatives being described as promising for the development of more potent anti-proliferative agents against PC-3 prostate cancer cells.¹⁰

Ligand-based virtual screening (LBVS) is based on the principle of similarity, where it defines that compounds with similar structures cause similar biological effects. This concept depends on one or a few experimentally identified “hits”. Research in large libraries of binders can then be efficiently performed in the search for similar compounds with chemical properties leading to known activities, resulting in the identification of potentially new active compounds.¹¹

The advancement of computational and theoretical chemistry methods, such as quantitative structure–activity relationships (QSAR) and structure–activity relationships (SAR) has further strengthened the ability to study the metabolism of new drugs in early discovery stage.¹² In the evolution of computational chemistry, the use of molecular modeling (MM) has been one of the most important advances in the design and discovery of new drugs. Currently, MM is an indispensable tool in not only the process of discovery, but also the optimization of existing prototypes and the rational design of new candidates.^{12,13}

Quantum chemistry techniques, SAR were used to minimize the energy of the chemical structure of the pivot compound *via* semi-empirical method (PM3), refined with basis set 6-31+G (d,p), calculated in the DFT level of theory B3LYP.¹⁴ Virtual screening based on the ligand was performed by shape and electrostatic similarity in five commercial compound libraries (DIVERSet-CL, DIVERSet-EXP)¹⁵(ZINC drug database, ZINC natural stock and Drug@FDA BindingDB).¹⁶ Pharmacokinetic and toxicological properties were predicted for the most promising compounds against prostate cancer PC-3. The contribution index of overlap with 50 % steric and electrostatic similarity of the structures

with the pivot was analyzed. Molecular docking of the selected compounds was performed to refine the search for new chemical entities that present better pharmacokinetic and toxicological properties and economical viability for use in the treatment of PC.

EXPERIMENTAL

Search of the bioactive structure of the vouacapan derivative

The derivative compound of vouacapan, 16-((diisobutylamino)methyl)-6 α -hydroxy-ivouacapane-7 β ,17 β -lactone (N,N-DHL, (3bS,5aR,6R,6aS,10aR,10bS,10cR)-2-[[bis(2-methylpropyl)amino]methyl]-3b,5a,6,6a,7,8,9,10,10a,10b,10c,11-dodecahydro-6-hydroxy-7,7,10a-trimethyl-4H-phenanthro[3,2b:10,1-b'.c']-difuran-4-one), described for the first time, with potent prostatic anti-cancer activity PC-3,¹⁰ in the absence of crystallographic structure necessitated the performance of bioactive conformation research of N,N-DHL. The present study was realized according to the methodology previously implemented by Hamdi *et al.*,¹⁴ who performed a quantum chemistry study of compounds of natural origin. The energy of minimization and 3D optimization of compound N,N-DHL was pre-optimized with the semi-empirical PM3 method and refined with the basis set 6-31+G (d,p) calculated in the DFT method through the B3LYP level of theory, in which polarized and diffuse functions are taken into account with Gaussian software 03, implemented in GaussView 5.0.¹⁷⁻¹⁹

The atomic charges used in this study were obtained with key word POP=CHELPG using the electrostatic potential.²⁰ With this strategy, it was possible to obtain the best potential quantum molecular series of points defined around the structure, and atomic charges offer the general advantage of being physically more satisfactory than Mulliken charges.²¹

Generation of a conformer library in databases

In this study, five commercial databases were used to perform the virtual screening step, *i.e.*, Chembridge DIVERSetTM-EXPRESS-PickTM Collection (DIVERSetTM-EXP), DIVERSet CORE Library (DIVERSetTM-CL), ZINC drug database, ZINC natural stock and Drug@FDA BindingDB, see Table S-I of the Supplementary material to this paper. For each molecule, 300 conformers were generated using the Merck Molecular Force Field MMFF94 implemented in OMEGA software (Open Eye Scientific Software, Santa Fe, NM, <http://www.eyesopen.com>), on a computer with Intel Core i7 2.4 GHz processor using Windows 7 Professional operating system. The voltage threshold (energy difference of the conformer data for the global minimum energy) was up to 9 kcal* mol⁻¹ and a mean square deviation (RMSD) of 0.6 Å.²²

Ligand-based virtual screening (LBVS) using the programs ROCS v2.4.1 and EON virtual screening via ROCS (shape similarity)

The databases ChemBridge DIVERSet, ChemBridge DIVERSet-Exp, ZINC drug database, ZINC natural stock and ZINC FDA BindingDB were screened *via* virtual screening using the ROCS program algorithm to generate and punctuate the three-dimensional database overlays with the reference structure of the N,N-DHL vouacapan derivative to obtain the Top2000 structures of each base, totaling 10,000.

Virtual screening via EON (electrostatic similarity)

The EON program calculated the Tanimoto electrostatic index of the structures of the 5 databases and the structure of N,N-DHL, besides calculating new partial loads for the input structures using MMFF94. The output files were grouped according to the score and the

* 1 kcal = 4184 J

results were classified based on the “ET_combo” analogous to “ComboTanimoto”.²³ At the end of the process, from the “Top2000/base”, only the “Top100/base” were selected, totaling 500 molecules.

Pharmacokinetic and toxicological properties predictions of the compounds studied

Prediction of pharmacokinetic properties. QikProp^{24,25} performs the prediction of pharmacokinetic properties using descriptors with less computational detachment. The program analyzes the chemical structure as a whole, not just fragments, and predicts the structure in three dimensions. The program can predict with great reliability a wide variety of properties. For each descriptor, in addition to the prediction, the program still provides a range of values taken as optimal. This range corresponds to values covering 95 % of the known drugs available in the program database. This server calculates pharmacokinetic properties: human intestinal absorption ($HIA\%$), cellular permeability, *Caco-2* (P_{Caco-2}), cell permeability Maden Darby canine kidney (P_{MDCK}), skin permeability (P_{skin}), plasma protein binding (PPB), penetration of the blood–brain barrier (c_{Brain}/c_{Blood}); among many others.^{26,27}

Toxicity prediction. The predictions of toxicity through the protocol “knowledge-based expert system”, were performed using Derek software. The protocol uses a virtual base of chemical structures and the respective reports of toxicity from the literature in order to analyze comparatively the chemical groups present in the studied structures.²⁸ The toxicities investigated were carcinogenicity, mutagenicity, genotoxicity, hepatotoxicity, teratogenicity and other. For each group with toxic potential present in the structure, the program generates an alert (probable, plausible, improbable, possible, certain, impossible, doubtful). Finally, a description is given of the potential toxicity of the complete structure, according to the logarithms of the program.²⁹

Selection of structures by similarity of 50 % steric and/or electrostatic overlap (50% ster/electr)

After selecting the structures with the best toxicity results, a molecular overlap assessment was performed using the program Discovery Studio Visualizer.³⁰ This technique allows the alignment of two or more structures based on specific criteria. The alignment of the structures was performed *via* the field adjustment method. The field alignment overlaps the structures maximizing the steric and/or electrostatic repulsion between atoms. In this study, the relative weight of the percentage contributions of the components in the force field estimation was adjusted to 50% ster/electr.

A target alignment option was set that considers only pairs of structures that have a single common target, the specific molecule in which all others will be aligned. Those that presented overlap similarity values greater than 75 % in the field alignment in 50% ster/electr were selected through this strategy for the subsequent step of determining binding affinities using molecular docking studies.

Molecular docking simulations study

Obtained from the protein data bank (PDB, <http://www.rcsb.org/pdb>)³¹ with the code PDB: 2OZ7 and resolution 1.8 Å for *Homo sapiens* organism. The reference ligand used was cyproterone acetate (CPA) in sdf format. This compound is a steroid anti-androgen used clinically in the treatment of prostate cancer. Compared with steroidal agonists for the androgen receptor (AR, for example, dihydrotestosterone, R1881), CPA is more bulky in structure and therefore apparently incompatible with the binding pocket observed in the crystalline X-ray structures of AR currently available for the ligand-binding domain (LBD). The ligand and protein structure for the docking were prepared using Discovery Studio 4.1 and DS

Viewer Pro 6.0 software,³² removing water molecules. The ligands for docking validations were obtained with crystallographic structures of the proteins, as well as the structure of CPA bound to the androgen receptor (*Homo sapiens*).³³

This molecular docking study was performed using the AutoDock 4.2 program³⁴ and the graphical interface PyRx (version 0.8.30).³⁵ AutoDock is a set of tools that allow the prediction of the interaction between ligand and macromolecule. To identify potential ligand–macromolecule combinations, the program has 3 options of algorithms: AS (simulated annealing), GA (genetic algorithm) and LGA (Lamarkian genetic algorithm)³⁴. In this study, LGA, which shows the best results in the search for the global minimum,³⁶ was used. The population size was 100, selection pressure 1.1, the number of operations was 10,000, the number of islands was 1 and the Niche size was 2, The weight of the operator to migrate was 0, mutated 100, and the crossing test was 100. The GRID coordinates were $x = 28.6324$, $y = -3.0075$ and $z = 2.8167$, from the pocket of interest that was chosen based on the interactions between amino acids, and a sphere of 10 Å radius was defined. Ten solutions were calculated for each ligand and the PyRx score was analyzed.

Molecular docking using AutoDock 4.2/Vina 1.1.2 and PyRx 0.8.30

For the docking study between AR and its specific ligand complexed (PDB code: 2OZ7), the coordinates used for 2OZ7 were $x = 26.9229$, $y = 1.3605$ and $z = 2.9661$; they were chosen according to the interaction between AR and its standard ligand CPA. The energy scoring function was used to evaluate the change of free energy of binding (ΔG) of interactions between the AR and the ligand through the PyRx 0.8.30. An analysis of the poses was also considered for the selection of the best binding energy by binding affinity calculations in AutoDock 4.2/Vina 1.1.2. The determination of the visualizations and distance of binding interactions with the binding pocket in AR were performed with Discovery Studio 4.1. The strategies used for virtual screening in this study are summarized in Fig. S-1 of the Supplementary material.

RESULTS AND DISCUSSION

Ligand- and structure-based virtual screening

In this phase of the virtual screening, the Top100 compounds of each base were selected, which progressed to the pharmacokinetic predictions using the Qikprop program, resulting in 366 structures with good pharmacokinetic behavior. This set went to the prediction stage of toxicity using the DEREK program. This analysis defined a set of 181 chemical structures. After these steps a refinement by similarity of overlap and contribution 50% ster/electr was performed, resulting in a set of 68 structures.

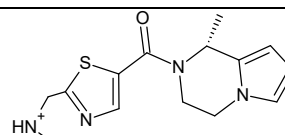
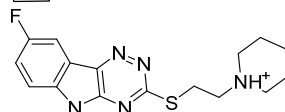
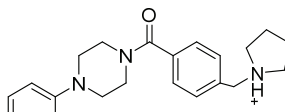
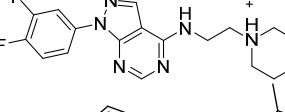
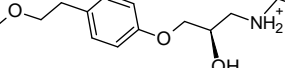
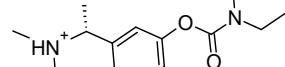
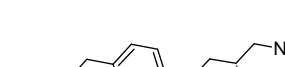
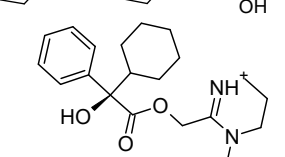
These structures advanced to docking in order to determine the binding affinity of them with the AR. At the end of this process, eight compounds with better results were obtained, the two largest values being displayed in Table I.

Pharmacokinetic and toxicity predictions studies

Several bioactive compounds did not reach the clinical trial stages due to adverse pharmacokinetic properties. Thus, it is essential to have access to pharmacokinetic profiles of potential drugs at the beginning of the planning, to verify

the possibility of future development.³⁷ A summary of twenty-one of the calculated ADME-related molecular descriptors based on the evaluation of metabolism and pharmacokinetics of drug resemblance profiles of the best structures are described in Table II.

TABLE I. Bioactive structures resulting from ligand- and structure-based virtual screening

No.	Bioactive structure	Code ID
1		Chembridge DIVERSet-CL 24665
2		Chembridge DIVERSet- EXP 18494
3		Chembridge DIVERSet- EXP 46104
4		Chembridge DIVERSet- EXP 44216
5		Drug@FDA BindingDB 61792
6		Drug@FDA BindingDB 50342600
7		Drug@FDA BindingDB 50404948
8		ZINC drug database 00057439

None of the structures showed any property with a value outside the recommended range for 95 % of known drugs (recommended range from 0 to 5).

Molecular weight is another parameter that influences the time of absorption. Thus, compounds with high molecular weight (above 500 Da) cross a membrane

TABLE II. Molecular properties calculated for the evaluation of metabolism and pharmacokinetic profiles of the main bioactive structures and recommended range for 95 % of known drugs; #stars^a = 0

No.	CNS ^b	MW ^c	SASA ^d	FOSA ^e	FTSA ^f	Vol ^g	LHD ^h	LHA ⁱ	log P ^j	Caco-2 ^k	log PBH ^l	MDCK ^m	P _{skin} ⁿ	#metab ^o	log K _{HSA^p}	PHOA ^q	PSA ^r
1	1	331.5	617.2	361.3	61.1	1076.5	0	6.5	2.58	650.9	0.259	515.33	-3.846	4	-0.123	92.03	48.80
2	1	346.5	629.9	338.2	53.8	1088.9	0	5.0	4.10	762.3	0.387	1202.3	-1.92	1	0.272	100	45.00
3	1	350.5	666.1	335.7	43.9	1194.9	0	6.0	4.10	945.9	0.343	515.4	-1.95	2	0.354	100	36.05
4	2	361.4	577.6	234.6	43.6	1036.6	1	7.2	2.92	952.7	0.541	1576.8	-2.85	3	-0.112	95.24	54.08
5	1	268.4	583.2	407.3	42.1	994.9	2	5.6	1.97	984.4	-0.052	538.1	-2.96	5	-0.205	91.64	49.28
6	1	251.4	548.5	401.2	37.8	935.1	0	5.0	2.78	1082.8	0.367	596.6	-2.28	3	-0.175	94.73	38.87
7	1	308.4	671.3	502.9	53.6	1165.2	2	5.6	2.80	767.1	-0.322	410.9	-2.61	5	0.126	100	48.78
8	0	345.5	648.3	432.6	60.1	1164.5	1	4.2	4.52	2667.7	-0.386	1428.8	-1.62	3	0.706	100	56.08
N,N- -DHL	1	472.7	764.4	649.6	85.7	1499.3	1	7.2	6.44	380.0	-0.292	192.3	-1.03	6	0.971	100	67.62

The number of calculated properties that are outside the range required for 95 % of known drugs (recommended range from 0 to 5); ^aactivity in the central nervous system on the scale -2 (inactive) to +2 (active); ^bmolar weight (recommended range: 130–725 Da); ^csolvent-accessible surface area (recommended range from 300.0 to 1000.0 Å²); ^dhydrophobic component of solvent-accessible surface area (recommended range from 0.0 to 750.0 Å²); ^ehydrophilic component of the solvent accessible surface area (recommended range from 7.0 to 320.0 Å²); ^ftotal volume of closed molecule per solvent-accessible molecular surface at Å³ (probe radius 1.4 Å, reach for 95 % of drugs: 500 to 2000 Å³); ^gnumber of hydrogen bonds donated by the molecule (range of 95 % of the drugs: 0 to 6); ^hnumber of hydrogen bonds accepted by the molecule (recommended range for drugs: 2–20); ⁱlogarithm of the partition coefficient between *n*-octanol and water phases (standard interval: -2 to 6.5); ^japparent permeability of the Caco-2 cell membrane on the Boehringer-Ingelheim scale, in nm s⁻¹ (range for 95 % of drugs: <5 low, >500 high); ^klogarithm of the penetration of the blood-brain barrier (CBlood–CBrain) (range for 95 % of drugs: -3.0 to 1.0); ^lthe apparent permeability of MDCK, in nm s⁻¹ (<25 poor, >500 optimum); ^mthe predicted skin permeability (recommended range: -8.0 to -1.0); ⁿnumber of metabolic reactions likely (recommended range: 1–8); ^ologarithm of the binding to human serum albumin (recommended range: -1.5 to 1.5); ^pthe predicted percentage of human oral absorption (>80 % high, <25 % poor); ^qvan der Waals surface area of polar nitrogen and oxygen atoms (recommended range: 7.0 to 200.0 Å²)^{38,39}

with difficulty, the lower the molecular weight is, the easier the compound crosses a lipid membrane.⁴⁰ CPA (positive control in this study), with 416.94 Da of molecular weight, shows rapid and almost total absorption in the body. Examples such as vancomycin, with a molecular weight of 1250 Da, also illustrates that reported above, because this drug does not present significant absorption when administered orally. Vancomycin tablets are employed to treat infections in the gastrointestinal tract, for systemic infections, the parenteral route is used. The structures that presented lower molecular weights were the compounds **6** (251.4 Da), **5** (268.4 Da) and **7** (308.4 Da) and are therefore more likely to exhibit high permeability and absorption in the body compared to the pivot compound N,N-DHL (negative control in this study) and the commercial drug CPA, widely used in the treatment of androgen-dependent prostate cancer.

The calculation of surface area accessible to the solvent (*SASA*) is a topological property, that makes it possible to quantitatively estimate the region excluded from contact with solvent at the interface between two molecules.⁴¹ The difference in the *SASA* of the structure with the smallest and largest value was only 122.8 Å², ranging from 548.5 (**6**) to 671.3 Å² (**7**), but still with smaller areas than the pivotal compound N,N-DHL (764.4 Å²). This reinforces the methodological success obtained and the promising character of the 8 structures selected in this research. These data make it possible to estimate the molecular surface and identify the interface-forming residues from the difference between the solvent accessible area (*SASA*) of the isolated protein and protein complexed with the studied ligands.

The hydrophilic component of the solvent accessible surface area (*FISA*) is the area of the atoms exposed to partial loads (in modulus) higher than 0.20e, while the hydrophobic component of the solvent accessible surface area (*FOSA*) is the exposed area due to other atoms.⁴¹ Structure **6** showed the lowest hydrophilic area of 37.8 Å², while **1** exhibited a *FISA* index of 61.1 Å², being the highest in the studied series. However, neither exceed the hydrophilic area 85.7 Å² of N,N-DHL, the negative control in this analysis. NH₂ and OH groups are considered hydrophilic and the exposed area of the NH₂ group is higher because there is an extra hydrogen atom and because the nitrogen atom has a greater radius than oxygen. Thus, the greater presence of these atoms in the selected structures could increase the hydrophilic area of the studied ligands. Compound **4** showed the lowest *FOSA* index 234.6 Å², while **7** showed the largest in the series, 502.9 Å². Therefore, relative to water, solvated molecule **4** was less unfavorable than solvated molecule **7**, but it is likely that the solubilization of both molecules in water was more favorable than of the negative control N,N-DHL and similar to the characteristics of CPA. Hence, it is estimated that the interface-forming residues of the complexed protein with the most promising ligands would have a hydrophobic profile, thus favoring better liposolubility

(desirable $\log P$), consequential interaction with the lipid membrane and increased binding affinity with the biological receptor. The interaction with the protein-binding pocket was visualized and the residues identified in this study through molecular docking simulations.

The total volume of the closed molecule per solvent-accessible molecular surface (Vol) is related to the relief of a particular molecular structure or sub-structure.⁴² Thus, compound **6** showed the smallest volume (935.1 \AA^3) from the series studied, whereas molecule **3** had the largest volume (1194.9 \AA^3), both significantly smaller than the volume of N,N-DHL (1499.3 \AA^3). Such facts suggest the promising behavior of the structures concerning solubility, interaction with the lipid layer and favorable coupling to the pocket of complexed protein binding.

The number of hydrogen bonds donated and bonds accepted by the molecule were low for all compounds, especially structures **6** and **7**, which presented desirable values for both properties, corroborating the results of the other properties and indicating a good profile of the candidates as new drugs. A large number of hydrogen bond donors and acceptors have been associated with poor membrane permeability due to the additional desolvation energy required to break hydrogen bonds when moving from an aqueous environment to the lipid membrane.⁴³

The molecular polar surface area (PSA), the surface belonging to polar atoms, is a descriptor that was shown to correlate well with passive molecular transport through membranes and, therefore, enables the transport properties of drugs to be predicted.⁴⁴ Compound **8** had the highest PSA index (56.08 \AA^2), compared to compound **6** (38.87 \AA^2), the lowest value of the series, such facts indicating good permeability of the molecule in a cellular lipid membrane. However, a low PSA ($PSA < 75 \text{ \AA}^2$) has been associated with an increased risk of adverse events due to non-specific toxicity, particularly when combined with high lipophilicity ($\log P > 4$).⁴⁵

A high PSA has been associated with poor membrane permeability and, in particular, with low blood–brain barrier penetration. For good oral bioavailability, an upper limit of 140 \AA^2 has been suggested, particularly when associated with a large number of rotatable bonds.⁴⁶

Using the Derek program, all toxicity warnings and their respective clusters in each surviving structure of the pharmacokinetic prediction filter were analyzed. A search was made for plausible, probable or certain alerts for toxicity such as carcinogenicity, mutagenicity, hepatotoxicity, teratogenicity and nephrotoxicity. The structures that at this stage presented undesirable results did not enter the subsequent stages of screening.

In the step of filtering by similarity of molecular overlap, between the structure of the pivot compound N,N-DHL and the remaining ligands of the toxicological prediction step, values for 50% ster/electr overlap similarity were deter-

mined and the results less than 75 % were excluded from advancing to the molecular docking stage. These data are described in Table III for only the two molecules considered the most promising in the best eight series.

TABLE III. Prediction of the pharmacokinetic properties and similarity index by overlap of the two most promising structures and the vouacapane derivative

Compound	Pharmacokinetic properties			Similarity overlap 50% ster/electr
	$\log P$	$\log PBH$	Caco-2	
N,N-DHL	6.44	-0.292	380.0	100
6	2.78	0.367	1082.8	81.96
7	2.80	-0.322	767.1	77.54

The blood–brain barrier is a specific structure that protects the central nervous system (CNS). It controls and regulates the homeostasis of the central nervous system through separation of the brain (brain) and systemic blood (blood). For a drug with biological activity in the CNS, a high penetration value is required. However, for a drug lacking CNS activity, as investigated here, a low penetration value is desired, to minimize side effects.^{47,48} For the structure **6** ($\log PBH^* = 0.367$), the values were higher than those presented by **7** ($\log PBH = -0.322$) and N,N-DHL ($\log PBH = -0.292$). The literature⁴⁹ suggests that PBH values less than 1 (brain/blood < 1) assign the molecule to the inactive status in the CNS. This indicates that structures with negative values did not show penetration into the CNS, which qualifies them as inactive in the CNS.

The Caco-2 cell model can be used in predictions of oral absorption of drugs by passive transport (transcellular and paracellular) in the organism of *Homo sapiens*.^{50,51} The use of this prediction model has grown in permeability and drug absorption assays. These models help in the development of structures with greater therapeutic potential, since they allow the prediction of the *in vivo* absorption, thereby identifying structures for screening before preclinical studies.^{52–58} The values of Caco-2 in ascending order for the structures were N,N-DHL (380.012), **7** (767.141) and **6** (1082.82). These values are directly related to the values of the other properties shown in Table III. The lowest indexes of similarity of 50% of ster/electr overlap among the structures belong to those with the highest value of Caco-2. This indicates that oral absorption by passive transport is favored in the non-steroidal bioactive compounds of this study.

The higher the $\log P$ value is, the more hydrophobic is the molecule. To achieve better permeability, the drug should have a moderate $\log P$ value (between 2 and 6.5). In this range, it is likely that there is a good balance between permeability and solubility.^{59–62}

The $\log P$ values show that the three bioactive compounds have higher affinity for the organic phase, being characterized as hydrophobic, in the descending

* $\log P c_{\text{Blood}} - c_{\text{Brain}}$

order N,N-DHL, **7** and **6**. All the bioactive compounds presented optimum log *P* values within the range favoring good permeability and solubility for drugs, with structure BindingDB50342600 being the most hydrophilic of the three compounds. The log *P* values are directly related to the values of 50% ster/electr and inversely related to the values of human oral absorption, *i.e.*, the lower the log *P* value for the three top compounds, the higher is the cell permeability value.

The results of analyzes of toxicity predictions demonstrate that none of the eight selected bioactive structures showed any toxicity alertness for the chosen activities: carcinogenicity, mutagenicity, hepatotoxicity, nephrotoxicity and teratogenicity. This reinforces the promising character of the final selected structures as future candidates for new drugs. In contrast, the structure of compound N,N-DHL showed a human hepatotoxicity alert, PLAUSIBLE for the group FURAN, suggesting that the ring may be responsible for the toxic action indicated for the pivot compound.

Molecular docking

Molecular docking studies enabled information related to the interactions between ligand and receptor to be obtained, which made possible the selection of the best binder possible in terms of the lowest binding affinity of the interaction. In the molecular docking step, 68 structures resulting from previous filtrations were used in 5 databases.

The comparison between the conformations of the crystallographic binder (complexed with AR and experimental values of crystallography) with the computational data resulting from redocking ($RMSD = 0.72$) showed that the parameters used in the docking protocol were representative.⁶³ $RMSD$ values below the reference level of 2.0 Å are considered by the literature to be of good quality.^{64,65}

The alignment between the conformations of experimental and computational origin, which qualitatively shows this result, is shown in Fig. 1.

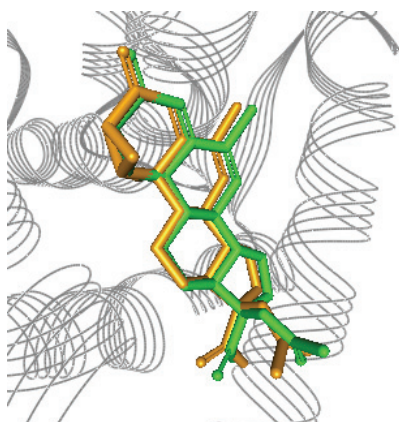


Fig. 1. Comparison between crystallographic ligand (green) and the best conformation resulting from molecular docking (golden).

The docking was used to select the most promising candidates for AR binding affinity. The bioactive compounds defined as the controls (black color) and their affinity values for this step were CPA ($-10.6 \text{ kcal mol}^{-1}$) and N,N-DHL ($-1.8 \text{ kcal mol}^{-1}$), contributing to the evaluation of the higher binding affinity compounds (colors blue and gray, respectively) are presented in Fig. 2.

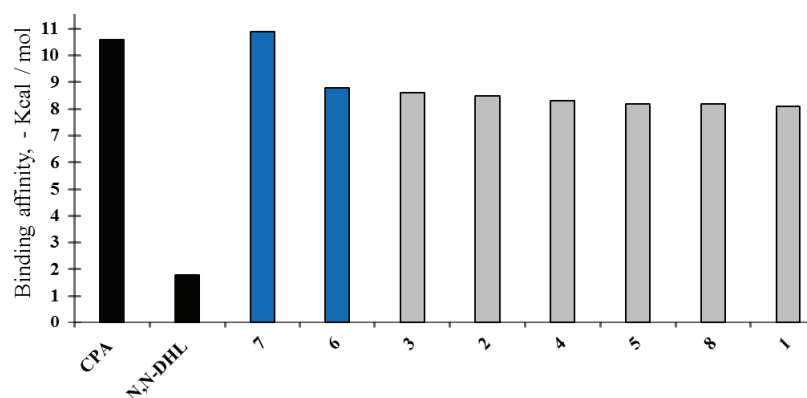


Fig. 2. Binding affinity provided by AutoDock/Vina software of the best candidates and AR.

The structures highlighted had values that varied between hits **7** ($-10.9 \text{ kcal mol}^{-1}$) as the best of the series, and **1** ($-8.1 \text{ kcal mol}^{-1}$) with a lower value. The other molecules were within this range of difference ($2.8 \text{ kcal mol}^{-1}$) with their respective values, **8** ($-8.2 \text{ kcal mol}^{-1}$), **5** ($-8.2 \text{ kcal mol}^{-1}$), **4** ($-8.3 \text{ kcal mol}^{-1}$), **2** ($-8.5 \text{ kcal mol}^{-1}$), **3** ($-8.6 \text{ kcal mol}^{-1}$) and **6** ($-8.8 \text{ kcal mol}^{-1}$).

All obtained good binding affinity values, indicating good interaction with AR, however two structures with better results were highlighted both from the base Drug_FDA_BindingDB (Fig. 2). One is the ligand **7**, which showed higher binding affinity than the commercial anti-cancer prostate drug, cyproterone acetate ($-10.6 \text{ kcal mol}^{-1}$) and the other triads.

The mean difference in binding affinity between the other compounds and CPA was low ($2.2 \text{ kcal mol}^{-1}$), but their values were more negative than that of the pivot N,N-DHL ($-1.8 \text{ kcal mol}^{-1}$), and hence, the molecule with second highest value **6** ($-8.8 \text{ kcal mol}^{-1}$) as a negative control over the CPA antagonist may be used in future acquisitions for *in vitro* biological assays, since the biological potency is inversely proportional to the binding affinity value of the compound, as described in previous research.⁶⁶ Therefore, this structure was separated from the set of other ligands that presented lower values, but very close to $-8.8 \text{ kcal mol}^{-1}$. The interactions of these structures are described below.

The interactions resulting from CPA docking with AR were: two hydrogen bonds with amino acids, one with ARG752 and one with ASN705, eight hydrophobic alkyl-type interactions distributed between MET (745, 787 and 895), LEU

(704 and 873), one VAL746 and two ALA877, in addition to three pi-alkyl interactions of TRP741, totaling thirteen interactions. The interactions of CPA with AR are shown in Fig. 3.

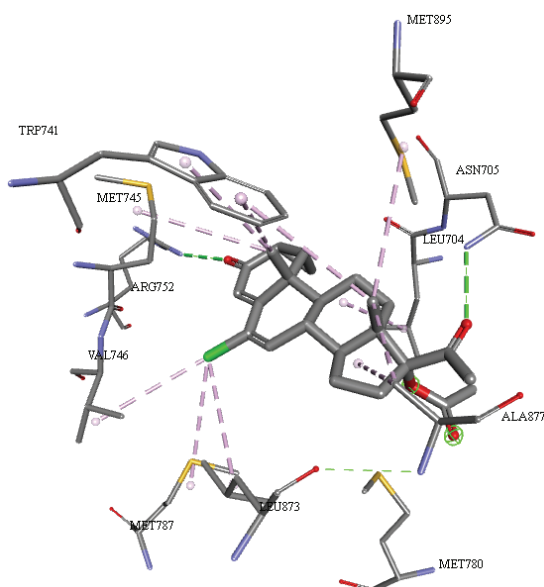


Fig. 3. Interactions between the CPA ligand and AR calculated by AutoDock 4.2.6.

The amino acids GLN711, MET780, MET745, ALA877 and LEU704 are shown in Fig. 4, which represents the binding pocket between the calculated AR and ligand, but only the last three form hydrophobic alkyl interactions. This demonstrates that the calculations were representative of the behavior of the AR-CPA complex taken from the PDB (2oz7 code). The ARG752 and ASN705 residues interact by hydrogen bonding with carbonyls, the former interacting with the carbonyl of the steroid skeleton, while in the AR-CPA complex (2oz7), the position is occupied by GLN711. MET780 binds to amino acid chains that interact directly with the ligand, suggesting some influence on affinity with the ligand, as illustrated in Fig. 4. It should be noted that the aromatic ring bound to the amino acid chain TRP741 performs interactions of the pi-alkyl type with the ligand, where one of these bonds is superimposed on another in Fig. 4.

Docking applied to molecules resulting from virtual screening

The interactions are shown in Fig. 5 for the structure of the synthetic N,N-DHL, as a nitrogen-hydrogen bond and another hydrophobic alkyl interaction with ALA877, similar to the amino acids LEU704 and LEU880 that exhibited three interactions each. MET745 and LEU707 each showed two further interactions of the same type, plus an interaction of MET780 with the ligand, *i.e.*, thirteen interactions in total.

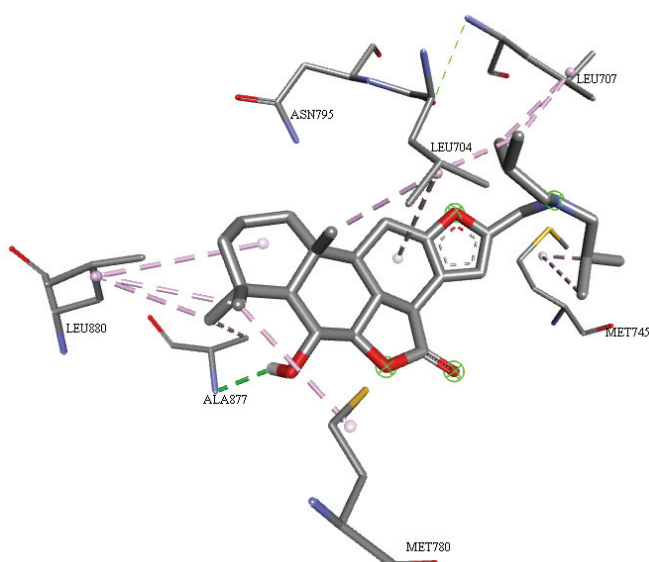


Fig. 4. Interactions between the N,N-DHL structure and the AR receptor calculated by AutoDock 4.2.6.

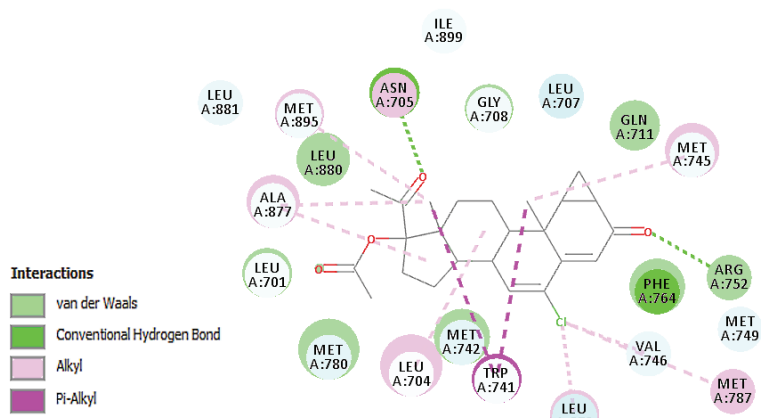


Fig. 5. 2D diagram of the pocket interactions between CPA and AR calculated in AutoDock 4.2.6.

It was possible in Fig. 6 to visualize completely all the amino acid chains that interact with the ligand in the docked AR binding pocket, as well as the exposure (light blue coloration) of the N,N-DHL atoms and amino acid residues to some solvent. TRP741 was not bound to the complexed vouacapan derivative but may influence it through the binding it makes with the amino acid LEU704, which directly interacts with one of the rings of the complexed steroid skeleton.

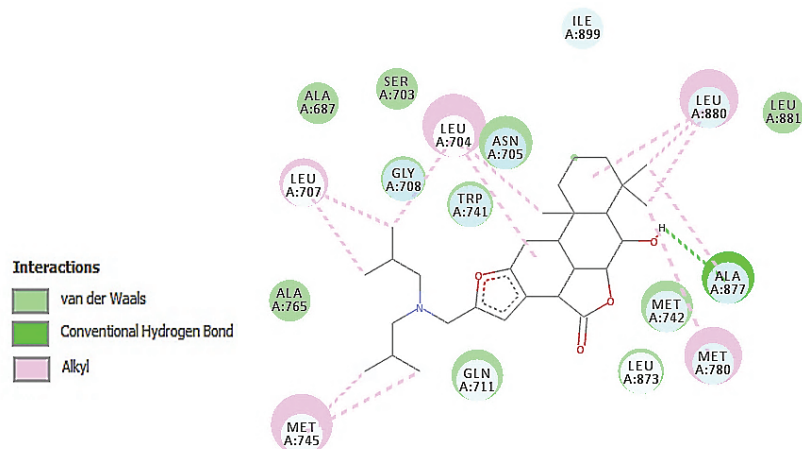


Fig. 6. 2D diagram of the pocket interactions between N,N-DHL and AR, calculated in AutoDock 4.2.6.

The structure of **6** showed a carbon–hydrogen bond with LEU873, four hydrophobic alkyl interactions distributed among the amino acids LEU704, LEU707, MET745 and MET749 with one interaction each, further interactions of the pi–alkyl type with LEU704 (one), PHE764 with two, plus MET742 with a pi–sulfur interaction, MET895 with a pi–sigma and TRP741 with a pi–pi interaction stacked with the aromatic ring of the ligand, *i.e.*, eleven interactions in total, as seen in Figs. 7 and 8.

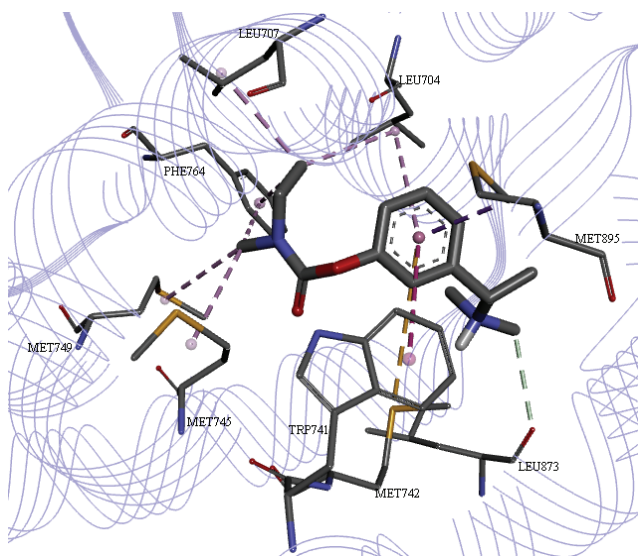


Fig. 7. Interactions between **6** and the AR receptor calculated by AutoDock 4.2.6.

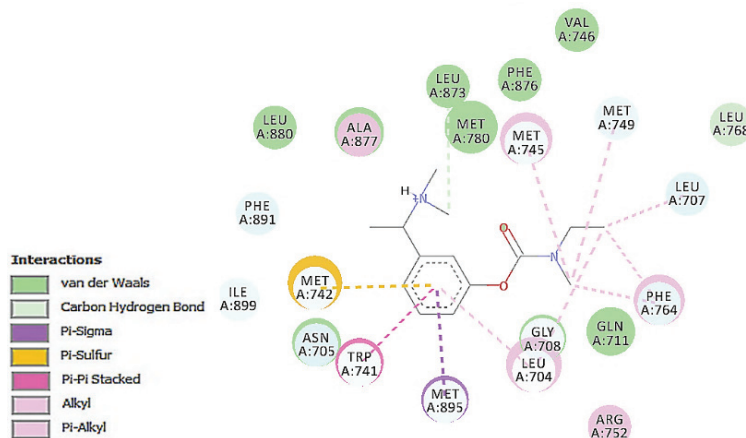


Fig. 8. 2D diagram of the pocket interactions between **6** and AR calculated in AutoDock 4.2.6.

Through the 2D diagram of the expanded visualization of the complexed bioactive compound of AR bonding, it was possible to verify the other amino acid chains that, although not bound to the compound, could indirectly influence the system through interactions with other amino acids that interact directly with the ligand, as shown in Fig. 8.

The structure of **7** interacts with receptor through a carbon–oxygen bond with MET745, a pi–cation interaction with the –NH₂ group of ARG752, three of a hydrophobic alkyl type, one for each amino acid LEU701, LEU704 and MET780, plus one pi–sigma interaction with MET742 and one pi–alkyl for LEU873 and another for ALA877, totaling eight interactions with AR, as shown in Figs. 9 and 10.

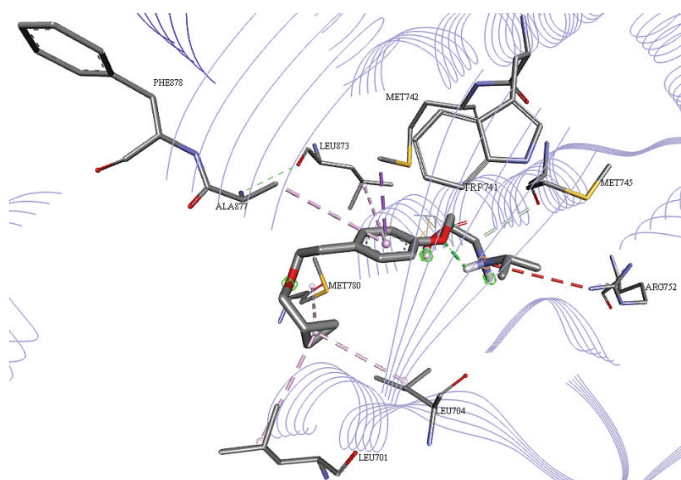


Fig. 9. Interactions between **7** and AR calculated through AutoDock 4.2.6.

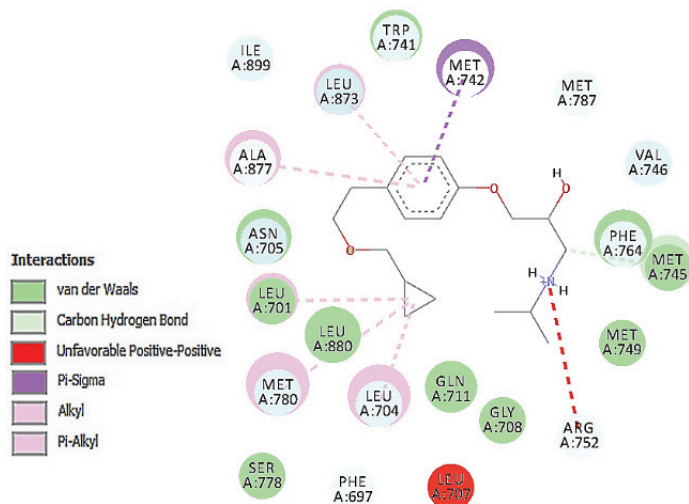


Fig. 10. 2D diagram of the binding pocket interactions between **7** and AR calculated in Autodock 4.2.6.

In Fig. 9, the presence of the amino acid TRP741 with the aromatic ring located near the aromatic nucleus of the compound is highlighted; this residue is bound to the residue MET742 that in turn interacts with the ligand ring through a hydrophobic pi-sigma interaction, very similar to the pi interaction that occurred between TRP741 and the aromatic ring of the **6** ligand.

Quantitative data on the binding distances and affinities between the ligands and AR are given in Table IV. It was verified that, between the structures CPA and N,N-DHL, the increased diversity of interactions with different amino acids might result in lower affinity binding, which indicates a higher degree of spontaneity of the interactions. This effect is noticeable in the structures **6** and **7** with eleven and eight interactions, respectively, and binding affinities with values smaller than the reference molecule N,N-DHL. Interactions with the amino acids LEU704 and MET745 occurred in all investigated structures, indicating that these residues may play a key role in their anti-prostate cancer activity (PC-3).

It is noted that the pi-sigma interactions MET895 (3.66 Å) and hydrogen bonding with LEU873 (3.23 Å) of the structure **6**, pi-sigma MET742 (3.74 Å) and carbon–oxygen bond MET745 (3.66 Å) from **7** may have influenced the higher values of the binding affinities obtained for these structures when compared to the interactions and binding affinity of AR with ligands that do not have hydrogen interactions with any of these amino acids.

Comparing the values of the binding affinities obtained for the two compounds, **6** ($-8.8 \text{ kcal mol}^{-1}$) and **7** ($-10.9 \text{ kcal mol}^{-1}$), the difference could be related to two exclusions of this bioactive structure, *i.e.*, a number of minor inter-

actions and the pi–cation bond with ARG752 at the position considered in the literature³³ and PDB code 2oz7, as important for the antagonistic action in AR.

TABLE IV. Distances, types of binding and affinities between the ligands and AR

Structure	Amino acid	Distance, Å	Interaction	Binding affinity, kcal mol ⁻¹
CPA	ARG752	3.19	Hydrogen bonding	-10.6
	ASN705	2.77	Hydrogen bonding	
	MET745	4.94	Hydrophobic alkyl	
	MET787	5.32	Hydrophobic alkyl	
	MET895	4.92	Hydrophobic alkyl	
	LEU873	5.32	Hydrophobic alkyl	
	LEU704	4.64	Hydrophobic alkyl	
	TRP741	5.36	Pi–alkyl	
	TRP741	4.81	Pi–alkyl	
	TRP741	5.20	Pi–alkyl	
	VAL746	4.43	Hydrophobic alkyl	
	ALA877	4.45	Hydrophobic alkyl	
	ALA877	4.64	Hydrophobic alkyl	
	ALA877	2.68	Hydrogen bonding	-1.8
	ALA877	3.65	Hydrophobic alkyl	
	LEU704	3.53	Hydrophobic alkyl	
	LEU704	3.94	Hydrophobic alkyl	
	LEU707	3.16	Hydrophobic alkyl	
	LEU707	3.60	Hydrophobic alkyl	
	LEU880	3.69	Hydrophobic alkyl	
	LEU880	4.02	Hydrophobic alkyl	
	MET745	3.92	Hydrophobic alkyl	
6	MET745	4.96	Hydrophobic alkyl	-8.8
	MET780	4.73	Hydrophobic alkyl	
	LEU704	4.43	Hydrophobic alkyl	
	LEU704	5.45	Pi–alkyl	
	LEU707	3.84	Hydrophobic alkyl	
	LEU873	3.23	Carbon–hydrogen bond	
	MET745	5.12	Hydrophobic alkyl	
	MET742	5.29	Pi–sulfur	
	MET895	3.53	Pi–sigma	
	MET749	5.03	Hydrophobic alkyl	
7	PHE764	4.75	Pi–alkyl	-10.9
	TRP741	5.48	Pi–Pi stacked	
	MET745	3.66	Carbon–oxygen bond	
	MET742	3.74	Pi–sigma	
	MET780	5.21	Hydrophobic alkyl	
	ARG752	5.41	Pi–cation	
	LEU701	4.91	Hydrophobic alkyl	
	LEU704	4.59	Hydrophobic alkyl	
	LEU873	5.03	Pi–alkyl	
	ALA877	5.50	Pi–alkyl	

The pi–cation interactions may exist between a positively charged atom (which has a formal charge of at least +0.5) and delocalized pi electrons, this allows the inclusion of delocalized cationic species, such as side chains of arginine.^{67,68} This indicates that the interaction with LEU704 and ARG752 may be a favorable factor for lowering binding affinity between these two structures. The interactions are strongly hydrophobic and when related to favorable entropic factors, may promote the lowering of the binding affinity between a linker and a receptor.⁶⁹

CONCLUSION AND FUTURE PERSPECTIVES

In this study, protocols were used for drug design based on a ligand and a structure, using optimization techniques on the chemical structure of a natural product vouacapane, virtual screening involving a total of 238,922 structures previously arranged in five commercial compound databases, pharmacokinetic prediction studies, toxicity, similarity by contribution of 50 % steric and electrostatic, and docking studies.

After molecular docking results for the bioactive structures derived from ligand-based virtual screening, it was proposed that the eight compounds selected in this study may bind to the androgen receptor with good binding affinity, highlighting the compounds **6** and **7**, as more potent and may be considered novel androgen receptor antagonist candidates. In addition, these promising structures could be used as prototypes for drug development *via* novel framework-based virtual screens or ligands in different databases for the search for novel antagonists with anti-prostate cancer activity and/or future acquisition and application of test protocol against the prostate cancer cell line PC-3.

Future studies of molecular modification of the resulting bioactive structure could also be performed with the aim of improving the binding affinity between the ligands (**6** and **7**) and AR protein to potentiate its antagonistic properties for prostate cancer.

Acknowledgements. We gratefully acknowledge the support provided by the PROPESP//FAPESPA/UFPA, CAPES for financial aid and the Institute of Exact and Natural Sciences of the Federal University of Pará (UFPA-Brazil) for the use of Gaussian software, as well as the Postgraduate Program in Medicinal Chemistry and Molecular Modeling (UFPA-Brazil), the Laboratory of Modeling and Computational Chemistry (LMCC) of the Federal University (UNIFAP-Brazil) and the Computational Laboratory of Pharmaceutical Chemistry (USP-Ribeirão Preto-Brazil) for computational support.

SUPPLEMENTARY MATERIAL

Virtual bases and predictions are available electronically from <http://www.shd.org.rs/JSCS/>, or from the corresponding author on request.

ИЗВОД

ВИРТУЕЛНИ СКРИНИНГ ЗАСНОВАН НА ЛИГАНДИМА И СТРУКТУРИ ЗА
16-((ДИИЗОБУТИЛАМИНО)МЕТИЛ)-6 α -ХИДРОКСВУАКАПАН-7 β ,17 β -ЛАКТОН,
ЈЕДИЊЕЊЕ СА ПОТЕНЦИЈАЛНОМ АКТИВНОШЋУ ПРОТИВ КАРЦИНОМА ПРОСТАТЕ

RAÍ C. SILVA^{1,2}, JOÃO G. C. POIANI³, RYAN S. RAMOS², JOSIVAN S. COSTA², CARLOS H. T. P. SILVA^{2,3},
DAVI S. B. BRASIL^{1,2} и CLEYDSON B. R. SANTOS^{1,2}

¹Postgraduate Program in Medicinal Chemistry and Molecular Modeling, Federal University of Pará, Rua Augusto Corrêa 01, 66075–110, Belém, Pará, Brazil, ²Laboratory of Modeling and Computational Chemistry, Federal University of Amapá, Rod JK Km 2, 68902–280, Macapá, Amapá, Brazil и ³Laboratory of Pharmaceutical Chemistry, Faculty of Pharmaceutical Sciences of Ribeirão Preto, University of São Paulo, Av. Prof. do Café, s/n - Monte Alegre, 14040-903, Ribeirão Preto, São Paulo, Brazil

Канцер простате је један од водећих узрока оболевања и смрти на планети. 16-((Дизобутиламино)метил)-6 α -хидроксивакапан-7 β ,17 β -лактон (N,N-DHL, стожер), једињење активно против канцера простате има вероватну биолошку активност на бази семијемпиријског (PM3) и рафинираног са базисним сетом 6-31+G(d,p) израчунавања DFT методом на B3LYP нивоу теорије. Ова структура је коришћена у на лиганду заснованом виртуалном скринингу за пет комерцијалних база једињења, коришћењем софтвера ROCS и EON који су одабрали 2000 односно 100 лиганада по бази. Овај сет је коришћен за фармакокинетичка и токсиколошка предвиђања. Индекс молекулског преклапања од 50 % стерног/електростатичког обезбедио је 68 структуре, за које је рађен молекулски докинг. Наши резултати показују да је од 238.922 структуре на крају одабрано осам: 7 ($-10,9 \text{ kcal mol}^{-1}$) као најбоља у серији, 1 ($-8,1 \text{ kcal mol}^{-1}$) као мање повољна, док су остале у овој области ($\pm 2,8 \text{ kcal mol}^{-1}$) са одговарајућим афинитетима везивања 8 ($-8,2 \text{ kcal mol}^{-1}$), 5 ($-8,2 \text{ kcal mol}^{-1}$), 4 ($-8,3 \text{ kcal mol}^{-1}$), 2 ($-8,5 \text{ kcal mol}^{-1}$), 3 ($-8,6 \text{ kcal mol}^{-1}$) и 6 ($-8,8 \text{ kcal mol}^{-1}$). Предвиђања за 21 фармакокинетичку особину су била унутар препорученог распона, са 95 % сличности са лековима доступним на тржишту и без упозорења на токсичност. Структуре имају сличност са N,N-DHL већу од 75 %. На основу предвиђања афинитета везивања, само се структуре 7 и 6 сматрају обећавајућим за потенцијалну активност против канцера простате (PC-3).

(Примљено 29. јануара, ревидирано 13. маја, прихваћено 29. маја 2018)

REFERENCES

1. T. C. A. Tonon, J. P. F. Schoffen, *Rev. Saude Pesqui* **2** (2009) 403
2. I. N. C. A. Estimativa de incidência de Câncer no Brasil 2016/ Instituto Nacional de Câncer José Alencar Gomes da Silva, Coordenação de Prevenção e Vigilância, Brazil, 2017, <http://www.inca.gov.br/estimativa/2016/> (Accessed June 18, 2017)
3. M. M. Center, A. Jemal, J. Lortet-Tieulent, E. Ward, J. Ferlay, O. Brawley, F. Bray, *Eur. Urol.* **61** (2012) 1079
4. R. Siegel, D. Naishadham, A. Jemal, *Ca-Cancer J. Clin.* **63** (2013) 11
5. R. L. Siegel, K. D. Miller, A. Jemal, *Ca-Cancer J. Clin.* **65** (2015) 05
6. D. M. Wilbert, J. E. Griffin, J. D. Wilson, *J. Clin. Endocrinol. Metab.* **56** (1983) 113
7. E. D. Crawford, *J. Urol.* **73** (2009) 4
8. J. C. Carvalho, J. A. Sertié, M. V. Barbosa, K. C. Patrício, L. R. Caputo, S. J. Sarti, L. P. Ferreira, J. K. Bastos, *J. Ethnopharmacol.* **64** (1999) 127
9. I. Carvalho, M. T. Pupo, A. D. L. Borges, L. S. Bernardes, *Quím. Nova* **26** (2003) 428
10. F. P. Euzébio, F. J. Dos Santos, D. Piló-Veloso, A. F. Alcântara, A. L. Ruiz, J. E. De Carvalho, M. A. Foglio, D. L. Ferreira-Alves, Â. De Fátima, *Bioorg. Med. Chem.* **18** (2010) 8172

11. P. Ripphausen, B. Nisius, J. Bajorath, *Drug. Discov. Today* **16** (2011) 372
12. N. Bruchovsky, P. S. Rennie, F. H. Batzold, S. L. Goldenberg, T. Fletcher, M. McLoughlin, *J. Clin. Endocrinol. Metab.* **67** (1988) 806
13. L. N. Thomas, R. C. Douglas, J. P. Vessey, R. Gupta, D. Fontaine, R. W. Norman, I. M. Thompson, D. A. Troyer, R. S. Rittmaster, C. B. Lazier, *J. Urol.* **170** (2003) 2019
14. O. A. A. Hamdi, E. H. Anouar, J. A. Shilpi, Z. B. K. A. Trabolsy, S. B. M. Zain, N. S. S. Zakaria, M. Zulkefeli, J. F. F. Weber, S. N. A. Malek, S. N. S. A. Rahman, K. Awang, *Int. J. Mol. Sci.* **16** (2015) 9450
15. ChemBridge, *The Gold standard in small molecule screening libraries and building blocks*, www.chembridge.com (Accessed Jun 22, 2017)
16. J. J. Irwin, B. K. Shoichet, *J. Chem. Inf. Model.* **45** (2005) 177
17. R. Dennington, T. Keith, J. Millam, *GaussView, Version 5*, Semichem Inc, Shawnee Mission, KS, 2009
18. *Gaussian 03, Revision C.02*, Gaussian, Inc., Wallingford, CA, 2004
19. *Gaussian 98: revision A. 7*, Gaussian, Inc., Pittsburgh PA, 1998
20. C. M. Breneman, K. B. Winberg, *J. Comput. Chem.* **11** (1990) 361
21. U. C. Singh, P. A. J. Kollman, *J. Comput. Chem.* **5** (1984) 129
22. P. C. D. Hawkins, A. Nicholls, *J. Chem. Inf. Model.* **52** (2012) 2919
23. Openeye Scientific Software. *EON, version 2.0.1*, Santa Fe, NM, 2007
24. Schrödinger Release 2019-1: QikProp, Schrödinger, LLC, New York, 2019
25. Schrödinger Release 2017-2: Maestro, Schrödinger, LLC, New York, 2017
26. T. Hou, J. Wang, *Expert Opin. Drug Metab. Toxicol.* **4** (2008) 759
27. N. S. R. Silva, D. J. L. Gonçalves, J. S. Silva, C. F. Santos, F. S. Braga, R. C. Silva, J. S. Costa, L. I. S. Hage-Melim, C. B. R. Santos, *Comput. Mol. Biosci.* **4** (2014) 47
28. C. A. Marchant, K. A. Briggs, A. Long, *Toxicol. Mech. Methods* **18** (2008) 177
29. N. Greene, P. N. Judson, J. J. Langowski, C. A. Marchant, *SAR QSAR Environ. Res.* **10** (1999) 299
30. DiscoveryStudio; INSIGHT, I. Accelrys Software Inc. San Diego, CA, 2009
31. H. M. Berman, J. Westbrook, Z. Feng, G. Gilliland, T. N. Bhat, H. Weissig, I. N. Shindyalov, P. E. Bourne, *Nucleic Acids Res.* **28** (2000) 235
32. DS Viewer PRO 6.0. Accelrys, Inc., San Diego, CA, 2005
33. C. E. Bohl, Z. Wu, D. D. Miller, C. E. Bell, J. T. Dalton, *J. Biol. Chem.* **282** (2007) 13648
34. G. M. Morris, R. Huey, W. Lindstrom, M. F. Sanner, R. K. Belew, D. S. Goodsell, A. J. Olson, *J. Comput. Chem.* **30** (2009) 2785
35. S. Dallakyan, A. J. Olson, *Methods Mol. Biol.* **1263** (2015) 243
36. G. W. Turner, E. Tedesco, K. D. Harris, R. L. Johnston, B. M. Kariuki, *Chem. Phys. Lett.* **321** (2000) 183
37. W. L. Jorgensen, E. M. Duffy, *Adv. Drug Deliv. Rev.* **54** (2002) 355
38. E. M. Duffy, W. L. Jorgensen, *J. Am. Chem. Soc.* **122** (2000) 2878
39. W. L. Jorgensen, E. M. Duffy, *Bioorg. Med. Chem. Lett.* **10** (2000) 1155
40. G. K. Zorzi, R. S. Schuh, A. M. D. Campos, E. L. Carvalho, M. B. Rott, H. F. Teixeira, *Quím. Nova* **40** (2017) 74
41. C. M. R. Sant'anna, *Quím. Nova* **25** (2002) 505
42. L. C. Tavares, *Quím. Nova* **27** (2004) 631
43. M. L. Connolly, *J. Appl. Crystallogr.* **16** (1983) 548
44. K. Palm, P. Stenberg, K. Luthman, P. Artursson, *Pharm. Res.* **14** (1997) 568
45. P. Ertl, B. Rohde, P. Selzer, *J. Med. Chem.* **43** (2000) 3714

46. J. D. Hughes, J. Blagg, D. A. Price, S. Bailey, G. A. Crescenzo, R. V. Devraj, E. Ellsworth, Y. M. Fobian, M. E. Gibbs, R. W. Gilles, N. Greene, E. Huang, T. Krieger-Burke, J. Loesel, T. Wager, L. Whiteley, Y. Zhang, *Bioorg. Med. Chem. Lett.* **18** (2008) 4872
47. H. Rojas, C. Ritter, F. D. Pizzol, *Rev. Bras. Terap. Intens.* **23** (2011) 222
48. J. Wang, T. Hou, *Ann. Rep. Comput. Chem.* **5** (2009) 101
49. X. Ma, C. Chen, J. Yang, *Acta Pharmacol. Sin.* **26** (2005) 500
50. S. Yamashita, T. Furubayashi, M. Kataoka, T. Sakane, H. Sezaki, H. Tokuda, *Eur. J. Pharm. Sci.* **10** (2000) 195
51. K. Horie, F. Tang, R. T. Borchardt, *Pharm. Res.* **20** (2003) 161
52. P. Artursson, C. Magnusson, *J. Pharm. Sci.* **79** (1990) 595
53. W. Rubas, N. Jezyk, G. M. Grass, *Pharm. Res.* **10** (1993) 113
54. M. J. Ginski, R. Taneja, J. E. Polli, *AAPS J.* **1** (1999) 27
55. K. A. Lentz, J. Hayashi, L. J. Lucisano, J. E. Polli, *Int. J. Pharm.* **200** (2000) 41
56. M. Kobayashi, N. Sada, M. Sugawara, K. Iseki, K. Miyazaki, *Int. J. Pharm.* **21** (2001) 87
57. S. Neulroff, A. L. Ungell, I. Zamora, P. Artusson, *Eur. J. Pharm. Sci.* **25** (2005) 211
58. J. De Souza, Z. M. F. Freitas, S. Storpirtis, *Rev. Bras. Cienc. Farm.* **43** (2007) 515
59. T. Fujita, J. Iwasa, C. Hansch, *J. Am. Chem. Soc.* **86** (1964) 5175
60. A. Leo, C. Hansch, D. Elkins, *Chem. Rev.* **71** (1971) 525
61. G. V. Betageri, J. A. Rogers, *Int. J. Pharm.* **36** (1987) 165
62. S. D. Krämer, *Pharm. Sci. Technol. Today* **2** (1999) 373
63. G. Jones, P. Willett, R. C. Glen, A. R. Leach, R. Taylor, *J. Mol. Biol.* **267** (1997) 727
64. U. Gowthaman, M. Jayakanthan, D. Sundar, *BMC Bioinf.* **9** (2008) S14
65. K. E. Hevener, W. Zhao, D. M. Ball, K. Babaoglu, J. Qi, S. W. White, R. E. Lee, *J. Chem. Inf. Model.* **49** (2009) 444
66. T. C. Lima, R. Lucarini, A. C. Volpe, C. Q. Andrade, A. M. Souza, P. M. Pauletti, A. H. Januário, G. V. Simaro, J. K. Bastos, W. R. Cunha, A. Borges, R. S. Laurentiz, V. A. Conforti, R. L. T. Parreira, C. H. G. Borges, G. F. Caramori, K. F. Andriani, M. L. A. Silva, *Bioorg. Med. Chem. Lett.* **27** (2017) 176
67. C. Biot, E. Buisine, J. M. Kwasigroch, R. Wintjens, *J. Biol. Chem.* **277** (2002) 40816
68. J. P. Gallivan, D. A. Dougherty, *Proc. Nat. Acad. Sci. U.S.A.* **96** (1999) 9459
69. J. M. Berg, J. L. Tymoczko, L. Stryer, *Biochemistry*, 5th ed., section 1.3, *Chemical Bonds in Biochemistry*, W. H. Freeman, New York, 2002, <https://www.ncbi.nlm.nih.gov/books/NBK22567/> (Accessed Dec 19, 2016).